Acta Cryst. (1996). B52, 668–676

Experimental Charge Density Study of 7-Dispiro[2.0.2.1]heptane Carboxylic Acid

DMITRII S. YUFIT,[a]* PAUL R. MALLINSON,[a] KENNETH W. MUIR,[a] SERGEI I. KOZHUSHKOV[b] AND ARMIN DE MEIJERE[b]

[a]*Department of Chemistry, University of Glasgow, Glasgow G12 8QQ, Scotland, and* [b]*Institut für Organische Chemie der Georg-August Universität, Göttingen D-37007, Germany. E-mail: dima@chem.gla.ac.uk*

(*Received 16 October 1995; accepted 22 January 1996*)

Abstract

The experimental charge density distribution in 7-dispiro[2.0.2.1]heptane carboxylic acid has been determined using single-crystal X-ray diffraction data measured at 100 K. Multipole refinement converged at $R = 0.023$ for 5539 reflections with $I \geq 3\sigma(I)$ and $\sin\theta/\lambda \leq 1.08$ Å^{-1}. Inclusion of hexadecapole functions for C atoms in the refinement is shown to be necessary. Experimental maps of the deformation density and of the Laplacian of ρ are in good agreement with those from *ab initio* calculations and also have some features specific for polyspirocyclopropanes. Analysis of the bond critical-point properties reveals that the effect of the π-acceptor hydroxycarbonyl substituent is more pronounced on the *endo*-side of the molecule, which can be related to the chemical behaviour of the compound. The influence of small conformational changes on the bond length distribution in the skeleton is also discussed.

1. Introduction

Highly strained small-ring molecules are of current interest to chemists. Papers on the nature of bonding even in the simplest strained molecule, cyclopropane, continue to appear (Karadakov, Geratti, Cooper & Raimondi, 1994; Inagaki, Ishitani & Kakefu, 1994). Recent progress in their synthesis, together with the development of experimental methods for the precise structure determination of such molecules, gives access to new experimental information for comparison with theoretical calculations, which are frequently not as precise for highly strained molecules as they are for unstrained species. Bader's topological theory of atoms in molecules (Bader, 1990) gives a new view on chemical bonding and its application to experimental X-ray crystallographic results both requires and greatly enhances the value of the multipole model of atomic density (Stewart, 1973). In the present paper we report the results of the multipole refinement of low-temperature single-crystal X-ray data for 7-dispiro[2.0.2.1]heptane carboxylic acid (1) and use the topological approach to describe the experimental charge density distribution.

The molecule (1) belongs to a relatively new class of small strained molecules – the polyspirocyclopropanes

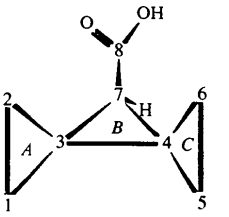

(1)

or triangulanes. The general approach to the very complicated synthesis of triangulanes was developed by Zefirov *et al.* (1990). Since then, systematic experimental studies of the structures of triangulanes and of the strained intermediates required for the synthesis have been started (Boese, 1992; Lukin, Kozhushkov, Zefirov, Yufit & Struchkov, 1993; Boese, Haumann, Eluvathingal, Kiran, Kozhushkov & de Meijere, 1996). As yet, only a few experimental charge density studies have been performed for triangulanes (Boese, Miebach & de Meijere, 1991; Irngartinger & Gries, 1991; Yufit, Antipin, Lukin, Struchkov & Zefirov, 1993) and for the determination of the deformation density distributions only the conventional *X–X* technique has so far been employed. These qualitative studies have revealed the features expected for three-membered rings: exocyclic shifts of the density peaks, the presence of relatively high charge density in the centres of the rings and the ellipticity of the bent bonds. Although these results enhanced understanding of the bonding in these compounds, they did not allow quantitative analysis of the effects of substituents and/or spiroconjugation. Experimental charge density studies using the multipole formalism are available for cyclopropane derivatives (Nijveldt & Vos, 1988; Koritsanszky, Buschmann & Luger, 1993), but not for triangulanes. Therefore, it was interesting to compare the results of a multipole refinement of (1) with those obtained earlier and to see if new information on the bonding in the molecule could be obtained from the topological properties of the experimental charge density.

2. Experimental

Compound (1) was synthesized by hydrolysis of the corresponding ethyl ester (de Meijere & Kozhushkov, 1995) and recrystallized from a $CCl_4/CHCl_3$ (1:1) mixture.

2.1. *Data collection*

Details of the data collection and refinement are given in Table 1. A transparent colourless crystal of (1) was mounted on a glass fibre and cooled slowly to 100 K on a Nonius CAD-4 diffractometer equipped with a Cryostream cooling unit. The cell dimensions were obtained by a least-squares fit to the setting angles of 24 reflections with $19 \leq \theta \leq 20°$. The data collection was carried out up to $\theta = 50°$ ($\sin\theta/\lambda \leq 1.08$ Å^{-1}). The intensities of all reflections ($-4 \rightarrow h \rightarrow 4$, $-8 \rightarrow k \rightarrow 8$, $-7 \rightarrow l \rightarrow 7$) were measured up to $\theta \leq 15°$ and those of the independent reflections ($-13 \rightarrow h \rightarrow 9$, $0 \rightarrow k \rightarrow 24$, $0 \rightarrow l \rightarrow 21$) up to 50° in θ. The results were used to choose the symmetrically related reflections with $I \geq 2\sigma(I)$ in the interval $15 \leq \theta \leq 50°$ and their intensities were also measured. The variations in the intensities of 4 control reflections during the data collection did not exceed 3%. The *DREAM* program package (Blessing, 1989, and references therein) was used for the data processing, scaling, profile analysis and merging of equivalent reflections. No extinction correction was applied since there was no indication that significant extinction was present. Absorption was also deemed to be insignificant.

2.2. *Refinement*

The positions of the C and O atoms were obtained by direct methods (*SHELXS*86; Sheldrick, 1985) and those of the H atoms from subsequent difference syntheses. Conventional refinement on F of the positional parameters of all atoms, of anisotropic displacement parameters for C and O atoms, and of isotropic ones for H atoms converged at $R = 0.0377$. This refinement revealed that the H atom of the carboxyl group was disordered. Each O atom in (1) is hydrogen-bonded to the O atom of a centrosymmetrically related molecule. Along each O···O vector peaks of similar height, corresponding to H atoms, were found at *ca* 0.9 Å from each O atom, suggesting that there is an equal probability that the H atom is bonded to each O atom. In the final cycles of conventional refinement the hydrogen disorder was therefore modelled by adjusting the positions and isotropic displacement parameters of both hydrogen sites, each of which was assigned a fixed occupancy of 1/2. The near equality of the U_{iso} parameters of the disordered H atoms [0.030 (2) and 0.029 (2) Å^2] provides some justification for this choice of site occupancy factor.

Although its most obvious manifestation is the presence of alternative sites for the carboxyl H atom, it is likely that disorder extends to the O and C atoms of the hydroxycarbonyl group. The electron density peaks corresponding to each of these atoms may well be a superposition of two peaks slightly displaced from one another, the observed electron density being an average of two possible structures. Nevertheless, we decided to persevere with a multipole refinement since (i) disorder did not appear to involve the feature of (1) of most interest, namely the triangulane skeleton, and (ii) the quality of the diffraction data seemed adequate to support such a refinement. It must be emphasized, however, that we do not suggest that the charge distribution in the hydroxycarbonyl group of (1) has been reliably determined by the calculations we now describe.

The carbon and oxygen parameters from the conventional refinement were used as starting values for the multipole refinement using the *XD* program package (Koritsanszky *et al.*, 1994). Both initially and after every multipole refinement cycle H-atom positions were normalized to give internuclear distances corresponding to the mean values derived from neutron diffraction (C—H 1.095, O—H 1.015 Å; Allen *et al.*, 1987).

During the multipole refinement the function $\Sigma w(|F_o| - k|F_c|)^2$ was minimized, where $w = 1/\sigma^2(F)$

Table 1. *Experimental details*

Crystal data	
Chemical formula	$C_8H_{10}O_2$
Chemical formula weight	138.17
Cell setting	Monoclinic
Space group	$P2_1/c$
a (Å)	6.386 (1)
b (Å)	11.264 (1)
c (Å)	10.105 (1)
β (°)	103.78 (1)
V (Å^3)	706.0 (1)
Z	4
D_x (Mg m^{-3})	1.300
Radiation type	Mo $K\alpha$
Wavelength (Å)	0.71073
No. of reflections for cell parameters	24
θ range (°)	19–20
μ (mm^{-1})	0.09
Temperature (K)	100.0 (3)
Crystal form	Prism
Crystal size (mm)	0.10 × 0.15 × 0.20
Crystal colour	Colourless
Data collection	
Diffractometer	Nonius CAD-4
Data collection method	ω–2θ
Absorption correction	Gaussian, see text
T_{min}	0.98
T_{max}	1.00
No. of measured reflections	11 899
No. of independent reflections	7085
No. of observed reflections	5539
Criterion for observed reflections	$I > 3\sigma(I)$
R_{int}	0.021
θ_{max} (°)	50
No. of standard reflections	4
Frequency of standard reflections	Every 120 min
Intensity decay (%)	3

Refinement

	N	R	wR	S
Spherical atom refinement	135	0.0377	0.0472	2.52
Multipole refinement				
Octapole level	299	0.0240	0.0261	1.42
Hexadecapole level	371	0.0227	0.0248	1.30

N = number of refined parameters; $R = \Sigma||F_o| - |F_c||/\Sigma|F_o|$; $wR = [\Sigma w(|F_o| - |F_c|)^2/\Sigma w|F_o|^2]^{1/2}$; $S = [\Sigma w(|F_o| - |F_c|)^2/(M - N)]^{1/2}$, where M is the number of observations.

and $\sigma^2(F) = \sigma_c^2 + (pIF^2)^2$ and $p = 0.010$ is the instrumental instability factor, which was determined from the fluctuations of intensity of the standard reflections and from the errors in the time-dependent scaling polynomials. The scattering factors were derived from wavefunctions tabulated by Clementi & Roetti (1974).

The rigid pseudo-atom model is now well established as the most effective tool for charge density studies and the basic equations of the formalism are readily accessible. In the present study we used the standard values of **n**: 2,2,2,3,4 for non-H atoms and 0,1,2,3,4 for H atoms. The ζ values were not optimized. During the refinement it was found that the expansion of the multipoles for the C atoms up to $l_{max} = 4$ (hexadecapoles) led to significant improvement of the model (see Table 1). However, the inclusion of hexadecapoles for O atoms in the refinement did not lead to any noticeable changes in the *R* and *S* values as well as in the deformation density maps. Accordingly, for O atoms $l_{max} = 3$. For H atoms the standard value $l_{max} = 1$ was used.

The contraction–expansion coefficients κ and κ' were refined for non-H atoms. For O atoms $\kappa = 0.990(2)$, $\kappa' = 0.92(4)$, for C atoms the corresponding values are 1.014(3) and 0.82(1). For H atoms fixed values of $k = k' = 1.16$ were used. No chemical or symmetry constraints were applied during the refinement.

Hirshfeld's rigid-bond test (Hirshfeld, 1976) was applied to the final thermal parameters. The maximum difference in the mean-square displacement amplitude for bonded atoms along the bond vector in (1) is 0.0007 Å^2, therefore, the final model is consistent with the rigid-bond hypothesis. Final atomic parameters are given in Tables 2 and 3.*

Table 2. *Fractional atomic coordinates and equivalent isotropic displacement parameters (Å^2)*

$U_{eq} = (1/3)\Sigma_i\Sigma_j U_{ij} a_i^* a_j^* \mathbf{a}_i.\mathbf{a}_j.$

	x	*y*	*z*	U_{eq}
O(1)	0.62988 (5)	0.96561 (3)	0.16458 (4)	0.016
O(2)	0.64329 (5)	0.87544 (3)	−0.03067 (3)	0.017
C(1)	1.26751 (4)	0.75054 (3)	0.18035 (3)	0.017
C(2)	1.16180 (4)	0.79982 (3)	0.03900 (3)	0.018
C(3)	1.03018 (4)	0.74961 (2)	0.12744 (2)	0.012
C(4)	0.85055 (4)	0.66975 (2)	0.11774 (2)	0.012
C(5)	0.80856 (5)	0.54807 (2)	0.16041 (3)	0.017
C(6)	0.70452 (5)	0.59415 (2)	0.01723 (3)	0.017
C(7)	0.83667 (4)	0.79125 (2)	0.17846 (2)	0.012
C(8)	0.69426 (4)	0.88241 (2)	0.09865 (2)	0.011

3. Results and discussion

3.1. *Molecular structure*

The molecular structure and labelling scheme of molecule (1) are shown in Fig. 1. Bond lengths and angles are given in Table 4. In general, the geometry of the triangulane frame shows the features expected from previous studies of triangulane derivatives – the elongation of distal bonds [C(1)—C(2) and C(5)—C(6)] and contraction of proximal bonds in terminal rings *A* and *C* [C(3)—C(1) and C(3)—C(2) in ring *A*], the strong contraction of the C—C bond between spiro nodes in ring *B*, which is accentuated by the π-acceptor substituent effect, and the corresponding distortion of bond angles. All the bond lengths are in agreement with the mean values for corresponding bonds given by Lukin, Kozhushkov, Zefirov, Yufit & Struchkov (1993), if Allen's δ^+ correction (−0.026 Å) for the electronic effect of the carbonyl-containing substituent (Allen, 1980) is taken into account. The disordering of the COOH group results in the equivalence of C—O bond lengths. Unexpected features of the molecular geometry of molecule (1) are the minor contraction of *endo*-proximal bonds C(2)—C(3) and C(4)—C(6) in terminal rings *A* and *C* compared with *exo*-bonds C(1)—C(3) and C(4)—C(5), and the different lengths of bonds C(3)—C(7) and C(4)—C(7) in the central ring *B*. The second feature may be the result of a slight deviation of the COOH group plane from the ideal position in which it bisects the angle C(3)—C(7)—C(4) [torsion angles C(3)—C(7)—C(8)—O(2) and C(4)—C(7)—C(8)—O(2) are 42.0(1) and −23.9(1)°, respectively], although the deviation amounts to a twist of only 9°. The difference in *exo*- and *endo*-bond lengths may be explained by some kind of remote effect of the substituent. A similar effect was noticed earlier (Yufit, Kozhushkov & de Meijere, 1995) during the structural study of another 7-carbonyldispiro[2.0.2.1]heptane derivative.

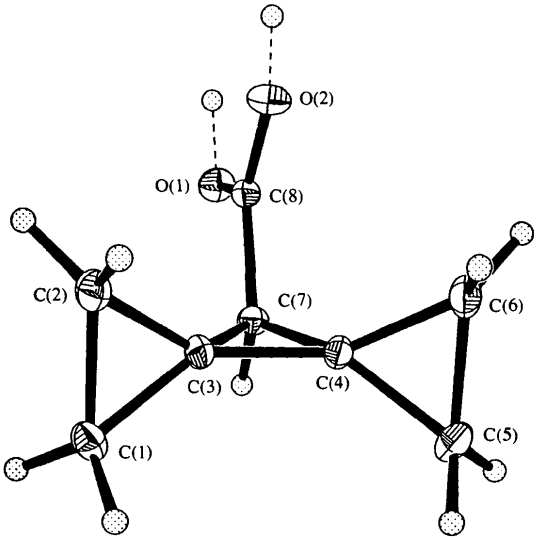

Fig. 1. The molecular structure and labelling scheme of molecule (1).

* Lists of multipole population coefficients and structure factors have been deposited with the IUCr (Reference: HA0142). Copies may be obtained through The Managing Editor, International Union of Crystallography, 5 Abbey Square, Chester CH1 2HU, England.

Table 3. *Anisotropic displacement parameters* ($Å^2$)

Atom	U_{11}	U_{22}	U_{33}	U_{12}	U_{13}	U_{23}
O(1)	0.0179 (11)	0.0128 (10)	0.0174 (11)	0.0032 (8)	0.0046 (9)	−0.0009 (8)
O(2)	0.0190 (12)	0.0212 (12)	0.0109 (9)	0.0042 (10)	0.0016 (8)	0.0023 (9)
C(1)	0.0099 (12)	0.0206 (11)	0.0181 (11)	−0.0005 (8)	0.0015 (7)	0.0016 (9)
C(2)	0.0135 (10)	0.0223 (12)	0.0168 (11)	−0.0039 (9)	0.0043 (8)	0.0030 (9)
C(3)	0.0093 (8)	0.0126 (9)	0.0143 (9)	−0.0011 (7)	0.0026 (7)	0.0007 (7)
C(4)	0.0110 (9)	0.0101 (8)	0.0138 (9)	−0.0013 (6)	0.0032 (7)	0.0005 (7)
C(5)	0.0187 (11)	0.0117 (9)	0.0206 (12)	−0.0004 (8)	0.0070 (9)	0.0034 (8)
C(6)	0.0171 (11)	0.0146 (10)	0.0170 (11)	−0.0049 (8)	0.0036 (8)	−0.0018 (8)
C(7)	0.0117 (9)	0.0116 (9)	0.0113 (8)	0.0009 (6)	0.0018 (6)	0.0006 (6)
C(8)	0.0110 (8)	0.0107 (8)	0.0114 (8)	0.0003 (6)	0.0016 (6)	0.0007 (6)

Table 4. *Selected geometric parameters* (Å, °)

O(1)—C(8)	1.273 (1)	C(3)—C(7)	1.522 (1)
O(2)—C(8)	1.272 (1)	C(4)—C(5)	1.480 (1)
C(1)—C(2)	1.531 (1)	C(4)—C(6)	1.475 (1)
C(1)—C(3)	1.482 (1)	C(4)—C(7)	1.511 (1)
C(2)—C(3)	1.477 (1)	C(5)—C(6)	1.532 (1)
C(3)—C(4)	1.443 (1)	C(7)—C(8)	1.477 (1)
C(2)—C(1)—C(3)	58.7 (1)	C(5)—C(4)—C(6)	62.4 (1)
C(1)—C(2)—C(3)	59.0 (1)	C(5)—C(4)—C(7)	133.5 (1)
C(1)—C(3)—C(2)	62.3 (1)	C(6)—C(4)—C(7)	135.6 (1)
C(1)—C(3)—C(4)	139.2 (1)	C(4)—C(5)—C(6)	58.6 (1)
C(1)—C(3)—C(7)	135.9 (1)	C(4)—C(6)—C(5)	59.0 (1)
C(2)—C(3)—C(4)	139.1 (1)	C(3)—C(7)—C(4)	56.8 (1)
C(2)—C(3)—C(7)	135.4 (1)	C(3)—C(7)—C(8)	118.2 (1)
C(4)—C(3)—C(7)	61.2 (1)	C(4)—C(7)—C(8)	119.7 (1)
C(3)—C(4)—C(5)	138.9 (1)	O(1)—C(8)—O(2)	123.2 (1)
C(3)—C(4)—C(6)	140.3 (1)	O(1)—C(8)—C(7)	117.4 (1)
C(3)—C(4)—C(7)	62.0 (1)	O(2)—C(8)—C(7)	119.4 (1)

In the crystal the molecules of (1) are held together as centrosymmetric dimers by pairs of O—H···O hydrogen bonds [O···O (1 − *x*, 2 − *y*, −*z*) 2.637 (1) Å] and are packed in a herringbone pattern, which is shown in Fig. 2. There are no other unusually short intermolecular contacts in the structure.

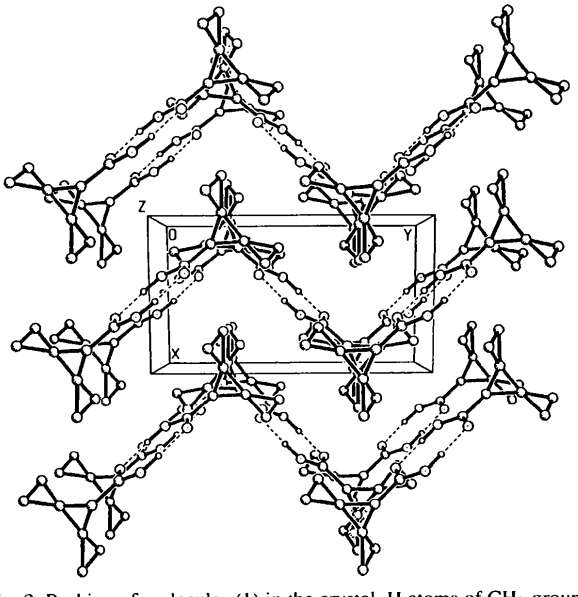

Fig. 2. Packing of molecules (1) in the crystal. H atoms of CH_2 groups omitted for clarity; 50% probability ellipsoids are shown for non-H atoms.

3.2. *Charge density distribution*

The residual density maps (Fig. 3) which show the discrepancies between multipole and observed structure factors, and indicate the quality of the model, do not have any peculiarities in the bond regions of the three-membered rings. The random distribution of the peaks and holes (from −0.13 to +0.14 e $Å^{-3}$) on the maps shows the satisfactory quality of the model. The largest positive peak lies in the middle of the C(8)—O(2) bond and is probably a result of the COOH group disordering mentioned above.

The static deformation density maps are presented in Figs. 4 and 5. The maps for the three cyclic fragments (Figs. 4*a–c*) show the same main features: the peaks are shifted ∼ 0.1 Å outside the internuclear vectors (bent bonds); there is a relatively high charge density in the centre of each ring; the high ellipticity of the terminal CH_2—CH_2 bonds is also evident from Fig. 4(*b*), where the peaks in the lower corners are the sections through the middles of these bonds. These features are well known and were found in other charge density studies of molecules containing three-membered rings. The shift of the peaks on the vicinal bonds in rings *A* and *C* toward the spiro nodes C(3) and C(4) is specific for (1). In both terminal rings the bridge of deformation density between the peaks on distal and *exo*-proximal [C(1)—C(3) and C(4)—C(5)] bonds is ∼ 0.2 e $Å^{-3}$ higher than that between the peaks on the distal bond and *endo*-proximal [C(2)—C(3) and C(4)—C(6)] bonds. The small ellipticity of the bonds in ring *B* (the peaks on the top of Figs. 4*a* and *c* are the cross sections of these bonds) is also rather unusual. The shape and intensity of the charge density maxima are well correlated with the bond lengths – the broad diffuse peaks on the long distal bonds C(1)—C(2) and C(5)—C(6), and also on the C(3)—C(7) bond, are distinguishable from the well shaped peaks (which are ∼ 0.3 e $Å^{-3}$ higher) on the shorter proximal bonds and especially on the C(3)—C(4) bond between two spiro atoms (*ca* 0.4 e $Å^{-3}$ higher). The interpretation of the deformation density distribution in the plane of the COOH group is complicated by the disorder, but the similarity of the charge distribution in the C—O fragments and the presence of diffuse peaks in the lone-pair regions of the O atoms is noticeable. The reason for the

significant difference in the C(3)—C(7) and C(4)—C(7) bond lengths is quite clear from the comparison of the charge density distributions in the C(3)—C(7)—C(8) and C(4)—C(7)—C(8) planes (Figs. 5*a* and *b*). The small torsional rotation of the carboxyl group around the C(7)—C(8) bond from the ideal bisecting position results in the predominant concentration of the charge of the carboxyl group in the latter plane, favouring conjugation along the C(8)—C(7)—C(4) chain at the expense of C(8)—C(7)—C(3).

3.3. *The Laplacian maps*

One of the main advantages of the multipole model is the possibility of analytical representation of the experimental charge density distribution. It gives an opportunity to calculate the Laplacian of the charge density, which indicates local concentrations and depletions of electronic charge. The Laplacian maps in the planes of the three-membered rings of (1) (Figs. 6*a–c*) show the presence of distorted circular regions of charge concentration around the centres of the rings. The maps in general correspond to those from the *ab initio* calculations of cyclopropane (Cremer & Kraka, 1985; Wiberg, Bader & Lau, 1987) and are in direct experimental support of the σ-aromaticity theory (Cremer & Kraka, 1985), which explains the unusual stability of cyclopropanes by charge delocalization into the ring plane. In comparison to these theoretical maps, the rings of negative Laplacian in (1) are narrower near the atomic nuclei and more distended in the bond regions. This may be a result of the smaller extent of σ-delocalization in the triangulanes compared with cyclopropanes due to the effect of spiro-conjugation and/or of the π-acceptor substituent. The Laplacian maps also show the difference between *endo-* and *exo*-C atoms in the terminal rings *A* and *C*: the charge concentrations in the CH_2 regions of *exo*-atoms C(1) and C(5) are much higher than those in the corresponding regions of the *endo*-atoms C(2) and C(6); for C(2) there is barely a negative Laplacian peak in this region. The absolute values of $-\nabla^2\rho$ in the critical points (CP) of these *exo*-C—C bonds are bigger than for *endo*-bonds (see Table 5) and that for C(4)—C(7) is bigger than the value for C(3)—C(7). It

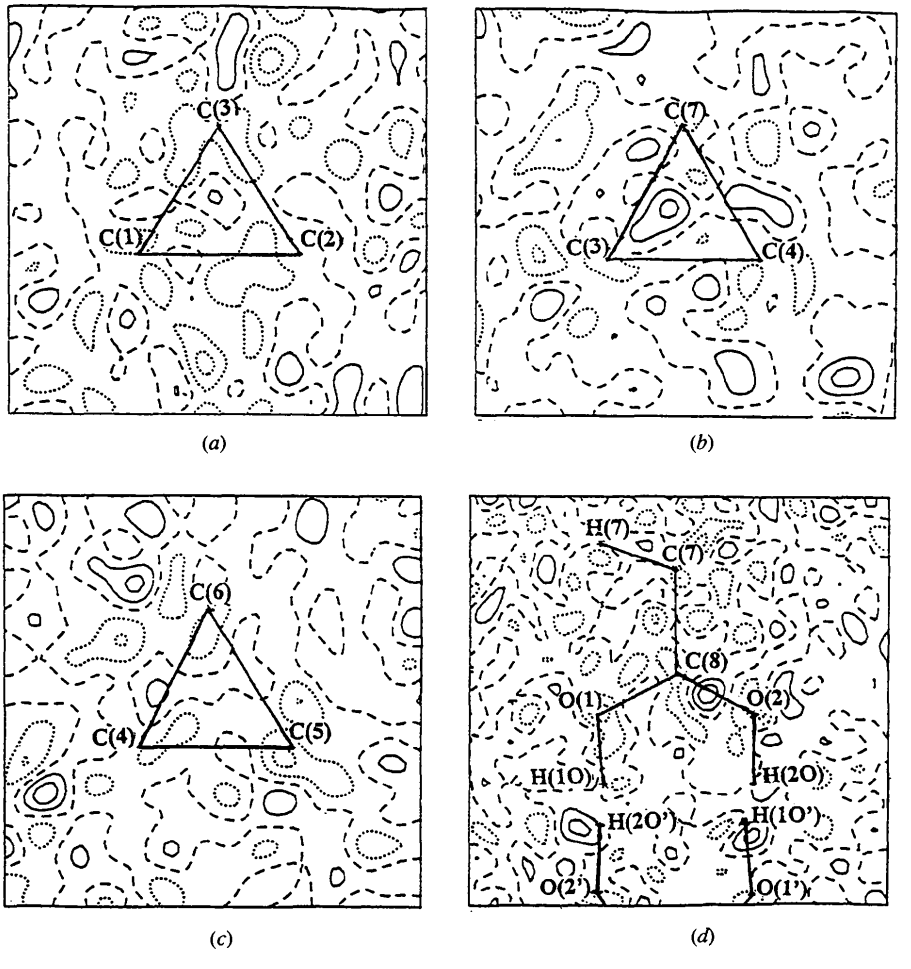

Fig. 3. Residual density maps in the planes (*a*) C(1)—C(2)—C(3), (*b*) C(3)—C(4)—C(7), (*c*) C(4)—C(5)—C(6) and (*d*) O(1)—O(2)—C(8). Contour intervals are 0.05 e Å^{-3}. Here and in Figs. 4–7 negative contours are shown as dotted lines.

must be noticed that the absolute values of the Laplacian for most of the C—C bonds in three-membered rings of (1) are higher than was calculated for C—C bonds in cyclopropane (12.8 e Å^{-5}; Cremer & Kraka, 1985; Wiberg, Bader & Lau, 1987) and spiropentane (12.1 e Å^{-5} for terminal, 13.8 e Å^{-5} for proximal bond; Wiberg, Bader & Lau, 1987). This may be a specific feature for triangulanes and other strained molecules in which there is a possibility of conjugation between the three-membered ring and substituents, because the corresponding values for bullvalene, which contains a cyclopropane ring with three unsaturated substituents, are also higher (19.8 e Å^{-5}; Koritsanszky, Buschmann & Luger, 1993). Thus, $-\nabla^2\rho$ values may be a sensitive indicator of the electronic interaction in the molecule and give additional information which cannot be obtained from deformation density maps.

3.4. *Critical point properties*

The properties of the full charge density at the critical points (the ellipticity, ϵ, of ρ and the absolute values of charge density and the Laplacian) and the positions of the points are among the most important characteristics of molecules according to Bader's theory of atoms in molecules (Bader, 1990). There are CP's of two types in (1) – (3,−1) bond CP's between bonded atoms and three (3,+1) ring CP's in the centres of three-membered rings. The properties of the CP's are given in Table 5. The values of the Laplacian in the bond CP's of molecule (1) were discussed earlier. The bond CP's for C—C bonds in three-membered rings are usually shifted radially outwards from the direct line between two bonded nuclei. Although this is normal for strained bonds, the magnitude of these shifts (**r**) and also the directions of the relative displacement (Δ, Table 5) of the CP towards one of the atomic centres may reflect the peculiarities of the electronic structure of the molecule. According to *ab initio* calculations for spiropentane (Wiberg, Bader & Lau, 1987) the CP's of proximal bonds are shifted along the C—C bond vectors away from the spiro atom towards the CH_2 group. This is the case for the terminal rings in (1), but not for the central ring where the direction of the shifts is towards spiro atoms, because of

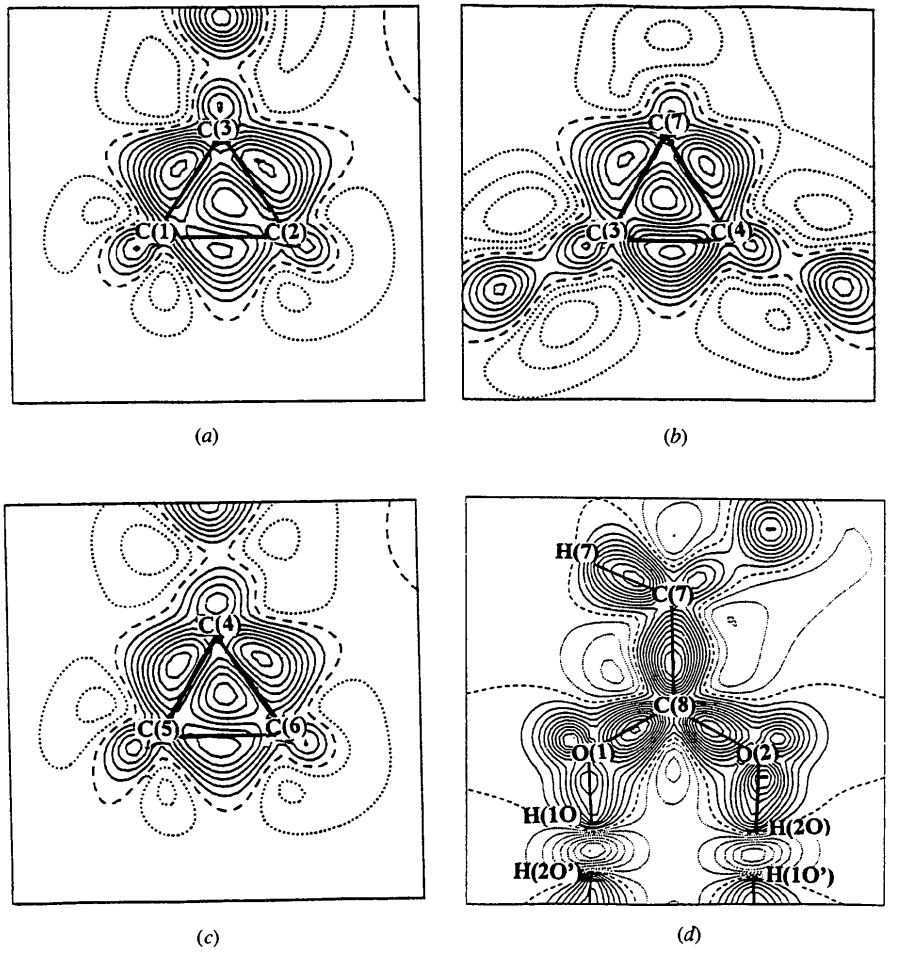

(*a*) (*b*) (*c*) (*d*)

Fig. 4. Static deformation density maps in the same planes as in Fig. 3. Contour intervals are 0.1 e Å^{-3}.

Table 5. *Some properties of the critical points*

Bond path	Type of CP	ρ (e Å^{-3})	$-\nabla^2\rho$ (e Å^{-5})	ε	Δ_{ij}*	r (Å)
O(1)—C(8)	(3,−1)	3.10 (5)	44.8 (3)	0.16	0.34	0.011
O(2)—C(8)	(3,−1)	3.10 (5)	47.0 (3)	0.14	0.32	0.016
C(1)—C(2)	(3,−1)	1.75 (4)	13.3 (1)	0.66	0.02	0.089
C(1)—C(3)	(3,−1)	2.10 (4)	20.8 (1)	0.44	−0.05	0.103
C(2)—C(3)	(3,−1)	2.00 (4)	16.4 (1)	0.25	−0.02	0.120
C(3)—C(4)	(3,−1)	2.15 (4)	17.9 (1)	0.12	−0.01	0.136
C(3)—C(7)	(3,−1)	1.77 (4)	11.0 (1)	0.28	−0.03	0.133
C(4)—C(5)	(3,−1)	2.06 (4)	20.2 (1)	0.29	0.03	0.089
C(4)—C(6)	(3,−1)	1.96 (4)	16.2 (1)	0.31	0.06	0.127
C(4)—C(7)	(3,−1)	1.92 (4)	16.8 (1)	0.21	−0.04	0.085
C(5)—C(6)	(3,−1)	1.73 (4)	11.9 (1)	0.53	0.00	0.091
C(7)—C(8)	(3,−1)	2.32 (4)	27.9 (1)	0.35	−0.12	0.011
C(1)—C(2)—C(3)†	(3,+1)	1.36 (4)	−8.6 (1)			
C(4)—C(5)—C(6)†	(3,+1)	1.32 (4)	−9.6 (1)			
C(3)—C(4)—C(7)†	(3,+1)	1.29 (4)	−12.8 (1)			

* The displacement of the CP from the bond midpoint is described by the parameters $\Delta_{ij} = (d_1 - d_2)/(d_1 + d_2)$ and **r**. The definitions of d_1, d_2 and **r** are obvious from the following figure:

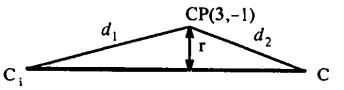

† Ring CP.

the strong effect of the carboxyl substituent. The shifts are dependent on the difference in atomic charges and for the highly polar C—O and C(7)—C(8) bonds, the magnitude of the relative displacements (Δ) is much higher (see Table 5). For the terminal C—C bonds and the central C(3)—C(4) bond, the shifts are negligible. The **r** values are systematically larger for *endo*-proximal bonds in terminal rings *A* and *C* than they are for *exo*-bonds and the absolute values of the **r** in the CP's are lower. These results provide additional evidence for transferance of the effect of the π-acceptor substituent through the spiro nodes, but the indications cannot be regarded as universal because for the central ring *B* the situation is different. In this ring **r** is larger and ρ is smaller for the longest C(3)—C(7) bond. The reason for the different bond CP properties in the central and terminal rings is not clear, but it may possibly be a result of the different electronic nature of the substituents of the rings. The conclusion which may be drawn is that in the triangulanes the interaction with the carboxyl group results in a decrease of the σ-delocalization in the three-membered rings. The C—O bonds in the disordered COOH group of (1) probably involve the superposition of single and double bonds, and their ellipticities are small and almost equal to each other. The very high ellipticity of the C(7)—C(8) bond is a result of strong interaction between the hydroxycarbonyl group and cyclopropane ring and was noticed earlier (Yufit, Antipin, Lukin, Struchkov & Zefirov, 1993) for the (1)-COOH isomer of acid (1).

All our experimental results indicate that the electronic properties of *endo*- and *exo*-CH_2 groups in the terminal rings are different. This implies a difference in the chemical behaviour of these groups. Unfortunately, the triangulanes are still rather exotic compounds and

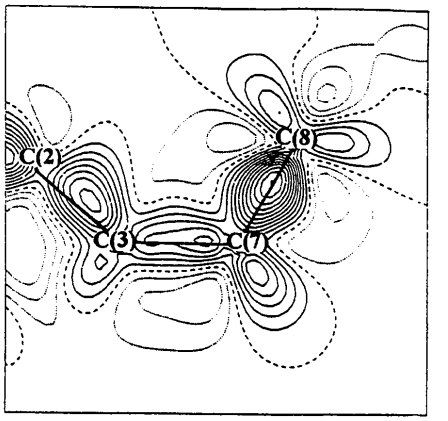

Fig. 5. Static deformation density maps in the planes (*a*) C(3)—C(7)—C(8) and (*b*) C(4)—C(7)—C(8). Contour intervals are 0.1 e Å^{-3}.

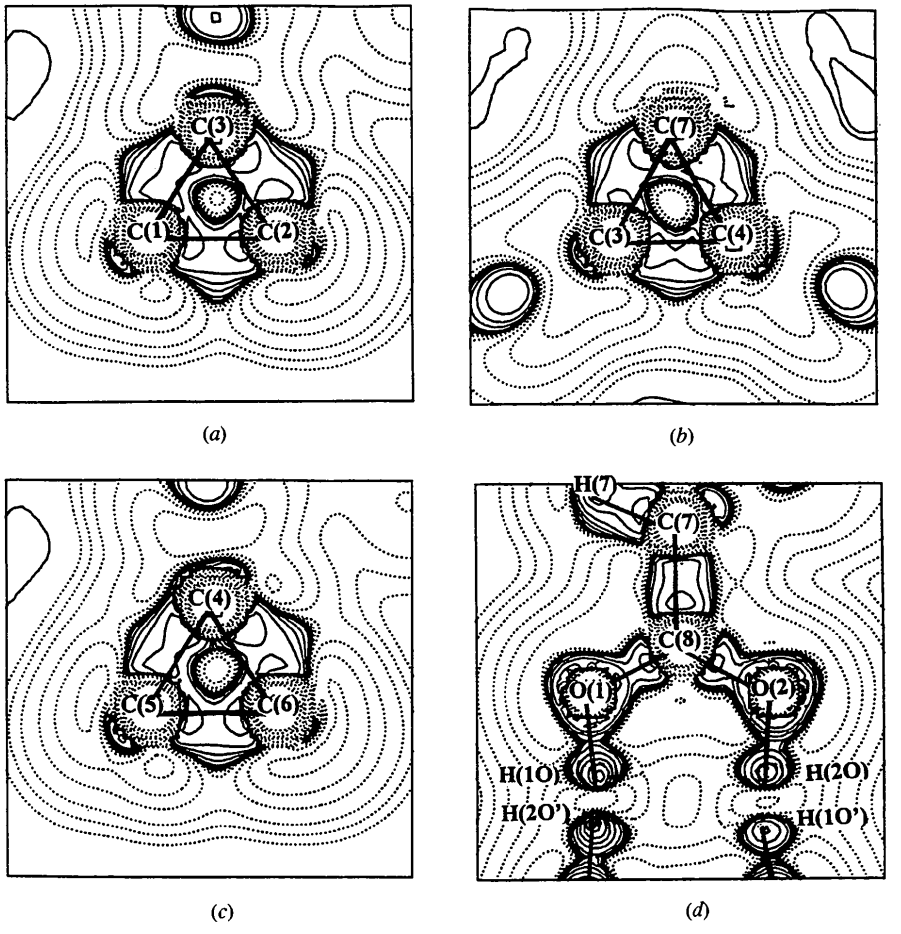

Fig. 6. The Laplacian maps in the same planes as in Figs. 3 and 4. Contours at logarithmic intervals in $-\nabla^2\rho$ e Å^{-5}.

their chemical properties have not yet been studied in detail. Nevertheless, Eaton & Lukin (1993), who discussed the amide activation of C—H bonds in triangulanes, have shown that stereospecific functionalization proceeds with the predominant formation of the *endo*-isomer. This is consistent with our conclusions on the different chemical properties of *endo*- and *exo*-CH_2 groups. However, these authors explained the regiospecificity by remote or through-space activation, whereas our results indicate that the influence of the acceptor substituent is transfered through the framework of C—C bonds.

4. Conclusions

This paper has shown that the application of topological theory to experimental multipole charge density studies provides important information on bonding in molecules which cannot be obtained from conventional *X–X* studies. Analysis of the experimental charge density distribution in terms of CP properties reveals new details of the molecular electronic structure and gives clues for the explanation of some chemical properties of triangulanes.

The authors are very thankful to Dr S. Howard (University of Wales, Cardiff) who helped us to solve some technical problems during the refinement. The authors are also grateful to the EPSRC for financial support.

References

Allen, F. H. (1980). *Acta Cryst.* B**36**, 81–96.
Allen, F. H., Kennard, O., Watson, D. G., Brammer, L., Orpen, A. G. & Taylor, R. (1987). *J. Chem. Soc. Perkin Trans. 2*, pp. S1–17.
Bader, R. F. W. (1990) *Atoms in Molecules – A Quantum Theory*. Oxford University Press.
Blessing, R. H. (1989). *J. Appl. Cryst.* **22**, 396–397.
Boese, R. (1992). *Advances in Strain in Organic Chemistry*, edited by B. Halton, Vol. 2, pp. 191–254. London: JAI Press Ltd.
Boese, R., Haumann, T., Eluvathingal, D. J., Kiran, B., Kozhushkov, S. I. & de Meijere, A. (1996). *Liebigs Ann.* In the press.
Boese, R., Miebach, T. & de Meijere, A. (1991). *J. Am. Chem. Soc.* **113**, 1743–1748.
Clementi, R. & Roetti, C. (1974). *At. Data Nucl. Data Tables*, **14**, 177–478.

Cremer, D. & Kraka, E (1985). *J. Am. Chem. Soc.* **107**, 3800–3810.

Eaton, P. E. & Lukin, K. A. (1993). *J. Am. Chem. Soc.* **115**, 11370–11375.

Hirshfeld, F. L. (1976). *Acta Cryst.* A**34**, 909–921.

Inagaki, S., Ishitani, Y. & Kakefu, T. (1994). *J. Am. Chem. Soc.* **116**, 5954–5958.

Irngartinger, H. & Gries, S. (1991). *Angew. Chem. Int. Ed. Engl.* **30**, 565–566.

Karadakov, P. B., Geratti, J., Cooper, D. L. & Raimondi, M. (1994). *J. Am. Chem. Soc.* **116**, 7714–7721.

Koritsanszky, T., Buschmann, J. & Luger, P. (1993). *Z. Naturforsch. Teil A*, **48**, 55.

Koritsanszky, T., Howard, S., Richter, T., Mallinson, P., Su, Z. & Hansen, N. (1994). *XD. A Computer Program Package for Multipole Refinement and Analysis of Charge Densities from Diffraction Data*. Berlin, Cardiff, Glasgow, Buffalo, Nancy.

Lukin, K. A., Kozhushkov, S. I., Zefirov, N. S., Yufit, D. S. & Struchkov, Yu. T. (1993). *Acta Cryst.* B**49**, 704–707.

Meijere, A. de & Kozhushkov, S. I. (1995). *Advances in Strain in Organic Chemistry*, edited by B. Halton, Vol. 4, pp. 225–282. London: JAI Press Ltd.

Nijveldt, D. & Vos, A. (1988). *Acta Cryst.* B**44**, 289–296.

Sheldrick, G. M. (1985). *SHELXS*86. *Program for the Solution of Crystal Structures*. University of Göttingen, Germany

Stewart, R. F. (1973). *J. Chem. Phys.* **58**, 1668.

Wiberg, K. B., Bader, R. F. W. & Lau, C. D. H. (1987). *J. Am. Chem. Soc.* **109**, 985–1001.

Yufit, D. S., Antipin, M. Yu., Lukin, K. A., Struchkov, Yu. T. & Zefirov, N. S. (1993). *Kristallografiya*, **38**(3), 78–84.

Yufit, D. S., Kozhushkov, S. I. & de Meijere, A. (1995). *Acta Cryst.* C**51**, 948–950.

Zefirov, N. S., Kozhushkov, S. I., Kuznetzova, T. S., Kokoreva, O. V., Ugrak, B. I., Lukin, K. A. & Tratch, S. S. (1990). *J. Am. Chem. Soc.* **112**, 7702–7707.